

# Theory of wakefields excited by an off-axis drive bunch in a plasma–dielectric waveguide

K.V. Galaydych,<sup>1,\*</sup> G.V. Sotnikov,<sup>1</sup> and I.N. Onishchenko<sup>1</sup>

<sup>1</sup>*NSC Kharkiv Institute of Physics and Technology, 61108 Kharkiv, Ukraine*

(Dated: March 7, 2022)

A linear theory of a wakefield excitation in a plasma–dielectric accelerating structure by a drive electron bunch in the case of an off-axis bunch injection has been constructed. The structure under investigation is a round dielectric–loaded metal waveguide with a channel for the charged particles, filled with homogeneous cold plasma. Derived theory was used to investigate numerically the spatial distribution of the bunch-excited wakefield components, which act on both the drive and witness bunches.

## I. INTRODUCTION

Among the advanced acceleration concepts it is possible to highlight four main schemes, namely: beam driven plasma wakefield acceleration, laser driven plasma wakefield acceleration, dielectric laser acceleration and structure based wakefield acceleration. The dielectric wakefield accelerating structures belong to the last one and for the present time a significant progress in their research and development has been made (see, for example, papers [1–3]). But despite the efforts and progress, there are the relevant tasks and problems that should be overcome. As for the conventional accelerators one of the severe issues of the advanced accelerators development is the beam breakup (BBU) instability of the drive bunch. This process is parasitic and leads to the bunch parameters degradation. Previous studies [4–11], devoted to as the transverse wakefields as BBU, highlight a strong importance of this problem, which has not been completely overcome at the moment. To control and suppress of this instability several methods have been proposed. Some of them are: (i) the BNS damping [12], which consist in variation of a betatron oscillation frequency along the bunch, (ii) a combination of a profiled quadrupole and FODO focusing system with an energy chirp of bunch [13, 14], (iv) excitation of a dielectric resonator by a train of bunches [15]. From other hand in the papers [16, 17] it was demonstrated that a plasma has the focusing properties and as a result it allows to focus a drive bunch. Authors of the paper [18] demonstrated, that a combination of a dielectric–loaded structure and plasma has an intrinsic focusing features and leads to the test and drive bunches to be focused. It was shown that in such a plasma–dielectric structure acceleration is provided by an eigenwave of the structure, and focusing is provided by a plasma wave. Therefore the aforementioned features of the plasma–dielectric structure allow to consider it as an alternative to a standard quadrupole focusing system and a possible way for the beam breakup mitigation during wakefield excitation and acceleration. This is the primary motivation of this paper.

## II. STATEMENT OF THE PROBLEM

The accelerating structure is a round dielectric–loaded metal waveguide with a channel for the charged particles. This channel is filled with homogeneous cold plasma. A relativistic drive electron bunch is injected with an offset into the plasma in parallel to the structure axis. The drive bunch passing through the structure excites wakefield. In the case of on-axis injection excited wakefield describes in terms of TM eigenmodes only. But due to the drive bunch offset the excited wakefield does not describe only in terms of TM eigenmodes and has all six components of the electromagnetic field. A three–dimensional general schematic of the plasma–dielectric accelerating structure with the drive bunch passing through are shown in Fig.1. The main goal of the paper is to construct a

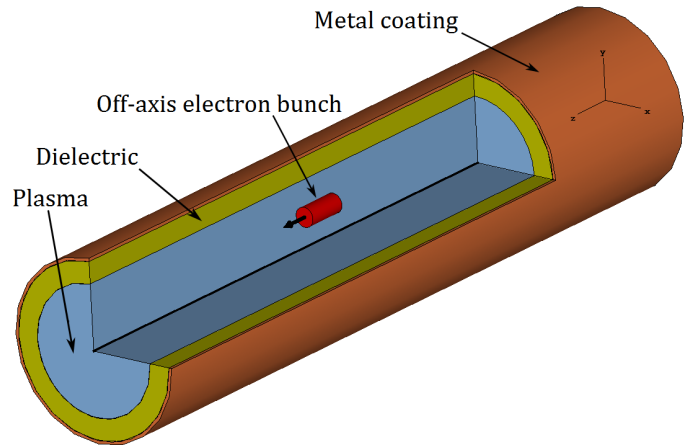


FIG. 1. General view of a round plasma–dielectric waveguide. A metal coating (orange), a dielectric (yellow), a plasma (blue) and an electron bunch (red) are shown schematically. An off-axis electron bunch moves in parallel to the axis.

linear theory of a wakefield excitation in the plasma–dielectric waveguide by the drive electron bunch in the case of an off-axis bunch injection taking into account high–order azimuthal modes.

\* [kgalaydych@gmail.com](mailto:kgalaydych@gmail.com)

### III. ANALYTICAL STUDIES

We start with the case of wakefield excited by a point-like charged particle (Green's function). For this particle of charge  $q$  moving with a constant velocity  $v$  along the waveguide axis ( $z$  direction) with the transverse coordinates  $r_0$  and  $\varphi_0$  the charge and current densities in the cylindrical coordinates are

$$\begin{aligned}\rho &= \frac{q}{v} \frac{\delta(r-r_0)}{r} \delta(\varphi-\varphi_0) \delta(t-t_0-z/v), \\ j_z &= q \frac{\delta(r-r_0)}{r} \delta(\varphi-\varphi_0) \delta(t-t_0-z/v),\end{aligned}\quad (1)$$

where  $t_0$  is an arrival time of the particle into the waveguide ( $z=0$ ), and  $\delta$  is the Dirac delta function. As we neglect the longitudinal boundedness effects we suppose that excited wakefield is defined by the source only. And therefore all the electromagnetic field components will depend on axial coordinate  $z$  and time  $t$  as the functions of a combination  $t-z/v$ . In this paper we do not take into account the transient process of electromagnetic field formation and group velocity effects associated with longitudinal boundedness of the practicable accelerating structures. The bunch-excited wakefield components, the charge and current densities can be expressed in terms of its Fourier transform in the variables  $t-z/v$  and  $\varphi$  as follows

$$\begin{aligned}\mathbf{E}(r, \varphi, \xi) &= \sum_{m=-\infty}^{+\infty} e^{im\varphi} \int_{-\infty}^{+\infty} d\omega \mathbf{E}_m^\omega(r, \omega) e^{-i\omega\xi}, \\ \mathbf{D}(r, \varphi, \xi) &= \sum_{m=-\infty}^{+\infty} e^{im\varphi} \int_{-\infty}^{+\infty} d\omega \varepsilon(\omega) \mathbf{E}_m^\omega(r, \omega) e^{-i\omega\xi}, \\ \mathbf{H}(r, \varphi, \xi) &= \sum_{m=-\infty}^{+\infty} e^{im\varphi} \int_{-\infty}^{+\infty} d\omega \mathbf{H}_m^\omega(r, \omega) e^{-i\omega\xi}, \\ \mathbf{B}(r, \varphi, \xi) &= \sum_{m=-\infty}^{+\infty} e^{im\varphi} \int_{-\infty}^{+\infty} d\omega \mu(\omega) \mathbf{H}_m^\omega(r, \omega) e^{-i\omega\xi}, \\ j_z(r, \varphi, \xi) &= \sum_{m=-\infty}^{+\infty} e^{im\varphi} \int_{-\infty}^{+\infty} d\omega j_{zm}^\omega(r, \omega) e^{-i\omega\xi},\end{aligned}\quad (2)$$

where  $\xi = t-z/v$ . The set of Maxwell's equations results to the system of the coupled equations for the Fourier transforms of the all field components:

$$\begin{aligned}\frac{m}{r} E_{zm}^\omega - \frac{\omega}{v} E_{\varphi m}^\omega &= \frac{\omega}{c} H_{rm}^\omega, \\ \frac{i\omega}{v} E_{rm}^\omega - \frac{\partial E_{zm}^\omega}{\partial r} &= \frac{i\omega}{c} H_{\varphi m}^\omega, \\ \frac{1}{r} \frac{\partial}{\partial r} (r E_{\varphi m}^\omega) - \frac{im}{r} E_{rm}^\omega &= \frac{i\omega}{c} H_{zm}^\omega, \\ \frac{m}{r} H_{zm}^\omega - \frac{\omega}{v} H_{\varphi m}^\omega &= -\frac{\omega\varepsilon(\omega)}{c} E_{rm}^\omega, \\ \frac{i\omega}{v} H_{rm}^\omega - \frac{\partial H_{zm}^\omega}{\partial r} &= -\frac{i\omega\varepsilon(\omega)}{c} E_{\varphi m}^\omega, \\ \frac{1}{r} \frac{\partial}{\partial r} (r H_{\varphi m}^\omega) - \frac{im}{r} H_{rm}^\omega &= \frac{4\pi}{c} j_{zm}^\omega - \frac{i\omega\varepsilon(\omega)}{c} E_{zm}^\omega.\end{aligned}\quad (3)$$

From the aforementioned equations it is possible to obtain the uncoupled wave equations for the Fourier transforms of the longitudinal electric and magnetic fields  $E_{zm}^\omega$ , and  $H_{zm}^\omega$ , namely:

$$\begin{aligned}\frac{1}{r} \frac{\partial}{\partial r} \left( r \frac{\partial E_{zm}^\omega}{\partial r} \right) - \frac{m^2}{r^2} E_{zm}^\omega - \frac{\omega^2}{v^2} (1 - \beta^2 \varepsilon(\omega)) E_{zm}^\omega &= \\ \frac{4\pi\omega i}{v^2} \frac{1 - \beta^2 \varepsilon(\omega)}{\varepsilon(\omega)} j_{zm}^\omega, \\ \frac{1}{r} \frac{\partial}{\partial r} \left( r \frac{\partial H_{zm}^\omega}{\partial r} \right) - \frac{m^2}{r^2} H_{zm}^\omega - \frac{\omega^2}{v^2} (1 - \beta^2 \varepsilon(\omega)) H_{zm}^\omega &= 0.\end{aligned}\quad (4)$$

All the other four Fourier transforms  $E_{rm}^\omega$ ,  $E_{\varphi m}^\omega$ ,  $H_{rm}^\omega$  and  $H_{\varphi m}^\omega$  can be expressed in terms of  $E_{zm}^\omega$ , and  $H_{zm}^\omega$ .

$$\begin{aligned}E_{rm}^\omega &= \frac{v}{\omega(1-\beta^2\varepsilon(\omega))} \left( \beta \frac{m}{r} H_{zm}^\omega - i \frac{\partial E_{zm}^\omega}{\partial r} \right), \\ E_{\varphi m}^\omega &= \frac{c\beta^2}{\omega(1-\beta^2\varepsilon(\omega))} \left( \frac{1}{\beta} \frac{m}{r} E_{zm}^\omega + i \frac{\partial H_{zm}^\omega}{\partial r} \right), \\ H_{rm}^\omega &= \frac{v}{\omega(1-\beta^2\varepsilon(\omega))} \left( -i \frac{\partial H_{zm}^\omega}{\partial r} - \beta \frac{m}{r} \varepsilon(\omega) E_{zm}^\omega \right), \\ H_{\varphi m}^\omega &= \frac{v}{\omega(1-\beta^2\varepsilon(\omega))} \left( \frac{m}{r} H_{zm}^\omega - i\beta\varepsilon(\omega) \frac{\partial E_{zm}^\omega}{\partial r} \right).\end{aligned}\quad (5)$$

To get the expressions for the Fourier transforms we should add the boundary conditions at the waveguide metal coating and at the plasma-dielectric interface. These boundary conditions are as follows: (I) at the waveguide wall ( $r=b$ ) the axial components of the electric field ( $E_{zm}^\omega$ ) should be equal zero, (II) at the plasma-dielectric interface ( $r=a$ ) the axial components of the electric field ( $E_{zm}^\omega$ ,  $E_{\varphi m}^\omega$ ), the axial components of the magnetic induction ( $B_{zm}^\omega$ ) and the radial components of the electric induction ( $D_{rm}^\omega$ ) should be continuous. The boundary conditions for the rest wakefield components will be satisfied automatically. In this paper we will omit the mathematical details and present the results for the axial components of electric and magnetic fields of any

given azimuthal  $m^{\text{th}}$  mode in the plasma and dielectric regions. A detailed description of the procedure for constructing the solutions for  $E_{zm}^\omega$  and  $H_{zm}^\omega$  can be found, for example, in the papers [4–6, 8]. The results which are satisfied aforementioned boundary condition are as follows:

$$\begin{aligned} E_{zm}^\omega(r < r_0) &= -\frac{iq}{\pi} \left( \frac{D_2(\omega)}{a\omega D(\omega)} \frac{I_m(\kappa_p r) I_m(\kappa_p r_0)}{I_m^2(\kappa_p a)} + \right. \\ &\quad \left. \frac{\kappa_p^2}{\omega \varepsilon_p(\omega)} \frac{I_m(\kappa_p r)}{I_m(\kappa_p a)} \Delta_m(\kappa_p a, \kappa_p r_0) \right) e^{-im\varphi_0 + i\omega t_0}, \\ E_{zm}^\omega(r > r_0) &= -\frac{iq}{\pi} \left( \frac{D_2(\omega)}{a\omega D(\omega)} \frac{I_m(\kappa_p r) I_m(\kappa_p r_0)}{I_m^2(\kappa_p a)} + \right. \\ &\quad \left. \frac{\kappa_p^2}{\omega \varepsilon_p(\omega)} \frac{I_m(\kappa_p r_0)}{I_m(\kappa_p a)} \Delta_m(\kappa_p a, \kappa_p r) \right) e^{-im\varphi_0 + i\omega t_0}, \\ E_{zm}^\omega(a < r < b) &= -\frac{iq}{\pi} \frac{D_2(\omega)}{a\omega D(\omega)} \frac{I_m(\kappa_p r_0)}{I_m(\kappa_p a)} \times \\ &\quad \frac{F_m(\kappa_d r, \kappa_d b)}{F_m(\kappa_d a, \kappa_d b)} e^{-im\varphi_0 + i\omega t_0}, \end{aligned} \quad (6)$$

$$\begin{aligned} H_{zm}^\omega(0 < r \leq a) &= \frac{q}{\pi} \frac{1}{a\omega D(\omega)} \frac{I_m(\kappa_p r) I_m(\kappa_p r_0)}{I_m^2(\kappa_p a)} \times \\ &\quad \beta \frac{m}{a} \frac{(\omega/v)^2 (\varepsilon_d - \varepsilon_p(\omega))}{\kappa_p^2 \kappa_d^2} e^{-im\varphi_0 + i\omega t_0}, \\ H_{zm}^\omega(a < r \leq b) &= \frac{q}{\pi} \frac{1}{a\omega D(\omega)} \frac{I_m(\kappa_p r_0)}{I_m(\kappa_p a)} \times \\ &\quad \beta \frac{m}{a} \frac{\Phi_m(\kappa_d r, \kappa_d b)}{\Phi_m(\kappa_d a, \kappa_d b)} \frac{(\omega/v)^2 (\varepsilon_d - \varepsilon_p(\omega))}{\kappa_p^2 \kappa_d^2} e^{-im\varphi_0 + i\omega t_0}, \end{aligned} \quad (7)$$

where the following notations are used:  $a$  is the inner radius of the dielectric,  $\kappa_p^2 = (\omega/v)^2(1 - \beta^2\varepsilon_p(\omega))$ ,  $\kappa_d^2 = (\omega/v)^2(\beta^2\varepsilon_d - 1)$ ,  $\Delta_m(x, y) = I_m(x)K_m(y) - K_m(x)I_m(y)$ ,  $I_m$  and  $K_m$  are the modified Bessel and Macdonald functions of the  $m^{\text{th}}$  order,  $\varepsilon_p(\omega) = 1 - \omega_p^2/\omega^2$  is the plasma permittivity,  $\omega_p$  is the plasma frequency,  $\varepsilon_d$  is the permittivity of the dielectric,  $F_m(x, y) = (-1)^m(J_m(x)Y_m(y) - Y_m(x)J_m(y))$ ,  $J_m$  and  $Y_m$  are the Bessel and Weber functions of the order  $m^{\text{th}}$ ,  $F'_m(x, y) = (-1)^m(J'_m(x)Y_m(y) - Y'_m(x)J_m(y))$ ,  $\Phi_m(x, y) = J_m(x)Y'_m(y) - Y_m(x)J'_m(y)$ ,  $\Phi'_m(x, y) = J'_m(x)Y'_m(y) - Y'_m(x)J'_m(y)$ . In the expressions (6) and (7) a function  $D(\omega)$  is a dispersion relation and it has the following form

$$\begin{aligned} D(\omega) &= D_1(\omega)D_2(\omega) - \frac{\beta^2 m^2 (\omega/v)^4}{a^2 \kappa_p^4 \kappa_d^4} (\varepsilon_d - \varepsilon_p)^2, \\ D_1(\omega) &= \frac{\varepsilon_p}{\kappa_p} \frac{I'_m(\kappa_p a)}{I_m(\kappa_p a)} + \frac{\varepsilon_d}{\kappa_d} \frac{F'_m(\kappa_d a, \kappa_d b)}{F_m(\kappa_d a, \kappa_d b)}, \\ D_2(\omega) &= \frac{1}{\kappa_p} \frac{I'_m(\kappa_p a)}{I_m(\kappa_p a)} + \frac{1}{\kappa_d} \frac{\Phi'_m(\kappa_d a, \kappa_d b)}{\Phi_m(\kappa_d a, \kappa_d b)}. \end{aligned} \quad (8)$$

The roots of the equation  $D(\omega) = 0$  define the frequencies of the plasma–dielectric waveguide eigenmodes, which are in Cherenkov resonance with the drive bunch. In the case of azimuthally homogenous eigenmodes ( $m = 0$ ) these frequencies are defined from the dispersion equation of the resonant  $TM$ -modes

$$\frac{\varepsilon_p(\omega)}{\kappa_p} \frac{I'_0(\kappa_p a)}{I_0(\kappa_p a)} + \frac{\varepsilon_d}{\kappa_d} \frac{F'_0(\kappa_d a, \kappa_d b)}{F_0(\kappa_d a, \kappa_d b)} = 0. \quad (9)$$

Inverse Fourier transform of the expressions (6) and (7) allows to obtain the distribution in space and time of the wakefield components excited by a point-like charged particle in the plasma–dielectric waveguide. It should be noted that expressions (6) and (7) have the simple poles  $\varepsilon_p(\omega) = 0$  and  $D(\omega) = 0$  only. The poles  $\varepsilon_p(\omega) = 0$  define the wakefield of plasma wave. The poles  $D(\omega) = 0$  define the wakefield of the plasma–dielectric eigenmodes, which are synchronous with the drive bunch, as was mentioned above. Performing inverse Fourier transforms with respect to the frequency with use of the calculus of residues as a result for the  $E_{zm}$  and  $H_{zm}$  we will obtain

$$\begin{aligned} E_{zm}(r < r_0, \varphi, \xi, r_0, \varphi_0, t_0) &= -2qk_p^2 \frac{I_m(\kappa_p r)}{I_m(\kappa_p a)} \times \\ &\quad \Delta_m(\kappa_p a, \kappa_p r_0) \cos \omega_p(\xi - t_0) \theta(\xi - t_0) e^{-im\varphi_0} - \\ &\quad \sum_{s=1} \frac{4qD_2(\omega_s)}{a\omega_s D'(\omega_s)} \frac{I_m(\kappa_{ps} r) I_m(\kappa_{ps} r_0)}{I_m^2(\kappa_{ps} a)} \times \\ &\quad \cos \omega_s(\xi - t_0) \theta(\xi - t_0) e^{-im\varphi_0}, \end{aligned} \quad (10)$$

$$\begin{aligned} E_{zm}(r_0 < r < a, \varphi, \xi, r_0, \varphi_0, t_0) &= -2qk_p^2 \frac{I_m(\kappa_p r_0)}{I_m(\kappa_p a)} \times \\ &\quad \Delta_m(\kappa_p a, \kappa_p r) \cos \omega_p(\xi - t_0) \theta(\xi - t_0) e^{-im\varphi_0} - \\ &\quad \sum_{s=1} \frac{4qD_2(\omega_s)}{a\omega_s D'(\omega_s)} \frac{I_m(\kappa_{ps} r) I_m(\kappa_{ps} r_0)}{I_m^2(\kappa_{ps} a)} \times \\ &\quad \cos \omega_s(\xi - t_0) \theta(\xi - t_0) e^{-im\varphi_0}, \end{aligned} \quad (11)$$

$$\begin{aligned} E_{zm}(a < r \leq b, \varphi, \xi, r_0, \varphi_0, t_0) &= -\sum_{s=1} \frac{4qD_2(\omega_s)}{a\omega_s D'(\omega_s)} \times \\ &\quad \frac{I_m(\kappa_{ps} r_0)}{I_m(\kappa_{ps} a)} \frac{F_m(\kappa_{ds} r, \kappa_{ds} b)}{F_m(\kappa_{ds} a, \kappa_{ds} b)} \cos \omega_s(\xi - t_0) \theta(\xi - t_0) e^{-im\varphi_0}, \end{aligned} \quad (12)$$

$$\begin{aligned} H_{zm}(0 < r \leq a, \varphi, \xi, r_0, \varphi_0, t_0) &= -\sum_{s=1} i \frac{4q\beta m}{a^2 \omega_s D'(\omega_s)} \times \\ &\quad \frac{I_m(\kappa_{ps} r) I_m(\kappa_{ps} r_0)}{I_m^2(\kappa_{ps} a)} \frac{(\omega_s/v)^2}{\kappa_{ps}^2 \kappa_{ds}^2} (\varepsilon_d - \varepsilon_p(\omega_s)) \times \\ &\quad \cos \omega_s(\xi - t_0) \theta(\xi - t_0) e^{-im\varphi_0}, \end{aligned} \quad (13)$$

$$\begin{aligned}
H_{zm}(a < r \leq b, \varphi, \xi, r_0, \varphi_0, t_0) = & - \sum_{s=1} i \frac{4q\beta m}{a^2 \omega_s D'(\omega_s)} \times \\
& \frac{I_m(\kappa_{ps}r)}{I_m(\kappa_{ps}a)} \frac{\Phi_m(\kappa_{ds}r, \kappa_{ds}b)}{\Phi_m(\kappa_{ds}a, \kappa_{ds}b)} \frac{(\omega_s/v)^2}{\kappa_{ps}^2 \kappa_{ds}^2} (\varepsilon_d - \varepsilon_p(\omega_s)) \times \\
& \cos \omega_s(\xi - t_0) \theta(\xi - t_0) e^{-im\varphi_0}, \tag{14}
\end{aligned}$$

In this paper we are mainly interested in the structure of the longitudinal and radial forces which act on the bunch particles. Therefore we present the expressions of the axial and radial components of the electric field, as well as the azimuthal component of the magnetic field only.

$$\begin{aligned}
E_{rm}(r < r_0, \varphi, \xi, r_0, \varphi_0, t_0) = & 2qk_p^2 \frac{I'_m(k_p r)}{I_m(k_p a)} \times \\
\Delta_m(k_p a, k_p r_0) \sin \omega_p(\xi - t_0) \theta(\xi - t_0) e^{-im\varphi_0} - & \\
\sum_{s=1} \frac{4q}{a\kappa_{ps}vD'(\omega_s)} \frac{I_m(\kappa_{ps}r_0)}{I_m^2(\kappa_{ps}a)} \times & \\
\left( \frac{m^2 \beta^2 k_s^2}{a\kappa_{ps}^2 \kappa_{ds}^2} (\varepsilon_d - \varepsilon_p(\omega_s)) \frac{I_m(\kappa_{ps}r)}{\kappa_{ps}r} - D_2(\omega_s) I'_m(\kappa_{ps}r) \right) \times & \\
\sin \omega_s(\xi - t_0) \theta(\xi - t_0) e^{-im\varphi_0}, & \tag{15}
\end{aligned}$$

$$\begin{aligned}
E_{rm}(r_0 < r < a, \varphi, \xi, r_0, \varphi_0, t_0) = & 2qk_p^2 \frac{I_m(k_p r_0)}{I_m(k_p a)} \times \\
\Delta'_m(k_p a, k_p r) \sin \omega_p(\xi - t_0) \theta(\xi - t_0) e^{-im\varphi_0} - & \\
\sum_{s=1} \frac{4q}{a\kappa_{ps}vD'(\omega_s)} \frac{I_m(\kappa_{ps}r_0)}{I_m^2(\kappa_{ps}a)} \times & \\
\left( \frac{m^2 \beta^2 k_s^2}{a\kappa_{ps}^2 \kappa_{ds}^2} (\varepsilon_d - \varepsilon_p(\omega_s)) \frac{I_m(\kappa_{ps}r)}{\kappa_{ps}r} - D_2(\omega_s) I'_m(\kappa_{ps}r) \right) \times & \\
\sin \omega_s(\xi - t_0) \theta(\xi - t_0) e^{-im\varphi_0}, & \tag{16}
\end{aligned}$$

$$\begin{aligned}
E_{rm}(a < r \leq b, \varphi, \xi, r_0, \varphi_0, t_0) = & \sum_{s=1} \frac{4q}{a\kappa_{ds}vD'(\omega_s)} \times \\
\frac{I_m(\kappa_{ps}r_0)}{I_m(\kappa_{ps}a)} \left( \frac{m^2 \beta^2 k_s^2}{a\kappa_{ps}^2 \kappa_{ds}^2} (\varepsilon_d - \varepsilon_p(\omega_s)) \frac{\Phi_m(\kappa_{ds}r, \kappa_{ds}b)}{\kappa_{ds}r \Phi_m(\kappa_{ds}a, \kappa_{ds}b)} - \right. & \\
\left. D_2(\omega_s) \frac{F'_m(\kappa_{ds}r, \kappa_{ds}b)}{F_m(\kappa_{ds}a, \kappa_{ds}b)} \right) \sin \omega_s(\xi - t_0) \theta(\xi - t_0) e^{-im\varphi_0} & \tag{17}
\end{aligned}$$

$$\begin{aligned}
H_{\varphi m}(0 < r \leq a, \varphi, \xi, r_0, \varphi_0, t_0) = & - \sum_{s=1} \frac{4q}{a\kappa_{ps}cD'(\omega_s)} \times \\
\frac{I_m(\kappa_{ps}r_0)}{I_m^2(\kappa_{ps}a)} \left( \frac{m^2 k_s^2}{a\kappa_{ps}^2 \kappa_{ds}^2} (\varepsilon_d - \varepsilon_p(\omega_s)) \frac{I_m(\kappa_{ps}r)}{\kappa_{ps}r} - \right. & \\
\left. \varepsilon_p(\omega_s) D_2(\omega_s) I'_m(\kappa_{ps}r) \right) \sin \omega_s(\xi - t_0) \theta(\xi - t_0) e^{-im\varphi_0} & \tag{18}
\end{aligned}$$

$$\begin{aligned}
H_{\varphi m}(a < r \leq b, \varphi, \xi, r_0, \varphi_0, t_0) = & \sum_{s=1} \frac{4q}{ca^2 \kappa_{ds}^2 D'(\omega_s)} \times \\
\frac{I_m(\kappa_{ps}r_0)}{I_m(\kappa_{ps}a)} \left( \frac{k_s^2}{\kappa_{ps}^2 \kappa_{ds}^2} (\varepsilon_d - \varepsilon_p(\omega_s)) \frac{\Phi_m(\kappa_{ds}r, \kappa_{ds}b)}{\Phi_m(\kappa_{ds}a, \kappa_{ds}b)} \frac{m^2}{r} - \right. & \\
\varepsilon_d \kappa_{ds} a D_2(\omega_s) \frac{F'_m(\kappa_{ds}r, \kappa_{ds}b)}{F_m(\kappa_{ds}a, \kappa_{ds}b)} \left. \right) \times & \\
\sin \omega_s(\xi - t_0) \theta(\xi - t_0) e^{-im\varphi_0}, & \tag{19}
\end{aligned}$$

where  $\kappa_{ps} = \kappa_p(\omega_s)$ ,  $\kappa_{ds} = \kappa_d(\omega_s)$ ,  $D'(\omega_s) = dD(\omega_s)/d\omega_s$ , and  $\theta$  is the Heaviside function. Expressions (10)–(19) describe a space–time structure of the wakefield excited by point–like charged particle injected with an offset in the waveguide under study. As it can be seen from the expressions (10), (11) and (15), (16) for the longitudinal and radial components of the electric field in the plasma region, the first terms describe the field of plasma wave. This field is potential and is localized in the plasma–filled channel for charged particles. The other terms describe the longitudinal and radial electric fields of the eigenwaves of the plasma–dielectric waveguide, respectively. The azimuthal component of the magnetic field does not contain the wakefield of the plasma wave. In the process of wakefield excitation the longitudinal dynamics of the bunch is determined by the axial component of the electric field ( $F_z/q = E_z$ ), and the radial dynamics is determined by the radial component of the Lorentz force, which is determined as  $F_r/q = E_r - \beta B_\varphi$ . In the plasma region expression for the  $F_r/q$  can be written as

$$\begin{aligned}
\frac{F_r(r < r_0, \varphi, \xi, r_0, \varphi_0, t_0)}{q} = & 2qk_p^2 \frac{I'_m(k_p r)}{I_m(k_p a)} \times \\
\Delta_m(k_p a, k_p r_0) \sin \omega_p(\xi - t_0) \theta(\xi - t_0) e^{-im\varphi_0} + & \\
\sum_{s=1} \frac{4q\kappa_{ps}vD_2(\omega_s)}{a\omega_s^2 D'(\omega_s)} \frac{I_m(\kappa_{ps}r_0) I'_m(\kappa_{ps}r)}{I_m^2(\kappa_{ps}a)} \times & \\
\sin \omega_s(\xi - t_0) \theta(\xi - t_0) e^{-im\varphi_0}, & \tag{20}
\end{aligned}$$

$$\begin{aligned}
\frac{F_r(r_0 < r \leq a, \varphi, \xi, r_0, \varphi_0, t_0)}{q} = & 2qk_p^2 \frac{I_m(k_p r_0)}{I_m(k_p a)} \times \\
\Delta'_m(k_p a, k_p r) \sin \omega_p(\xi - t_0) \theta(\xi - t_0) e^{-im\varphi_0} + & \\
\sum_{s=1} \frac{4q\kappa_{ps}vD_2(\omega_s)}{a\omega_s^2 D'(\omega_s)} \frac{I_m(\kappa_{ps}r_0) I'_m(\kappa_{ps}r)}{I_m^2(\kappa_{ps}a)} \times & \\
\sin \omega_s(\xi - t_0) \theta(\xi - t_0) e^{-im\varphi_0} & \tag{21}
\end{aligned}$$

In order to get wakefield excited by a drive bunch of finite size, it is necessary to integrate the expressions for the point–like particle over the arrival time  $t_0$  and by the transverse coordinates  $r_0$ , and  $\varphi_0$ . For the sake of simplicity we suppose that: (I) the drive bunch has a square profile of the charge density in both longitudinal

and transverse directions (uniform distribution), (II) the bunch offset  $R_{off}$  is more than drive bunch radius  $R_b$ . The resulting expressions for the axial and radial forces which act as on a witness bunch as on the drive bunch peripheral particles located near the plasma–dielectric interface ( $r = R_{off} + R_b$ ), and near the accelerating structure axis ( $r = R_{off} - R_b$ ) look like

$$\begin{aligned} \frac{F_z(r = R_{off} + R_b, \varphi, \xi)}{q} &= -\frac{4Q_b}{R_b L_b} \sum_{m=-\infty}^{+\infty} e^{im\varphi} \times \\ &\left( \frac{I_m(k_p R_{off}) I_1(k_p R_b)}{I_m(k_p a)} \Delta_m(k_p a, k_p (R_{off} + R_b)) \Psi_{\parallel}^{(p)}(\xi) + \right. \\ &\sum_{s=1} \frac{2v D_2(\omega_s)}{a \kappa_{ps} \omega_s^2 D'(\omega_s)} \frac{I_m(\kappa_{ps} R_{off}) I_1(\kappa_{ps} R_b)}{I_m^2(\kappa_{ps} a)} \times \\ &\left. I_m(\kappa_{ps} (R_{off} + R_b)) \Psi_{\parallel}^{(s)}(\xi) \right) \end{aligned} \quad (22)$$

$$\begin{aligned} \frac{F_r(r = R_{off} + R_b, \varphi, \xi)}{q} &= \frac{4Q_b}{R_b L_b} \sum_{m=-\infty}^{+\infty} e^{im\varphi} \times \\ &\left( \frac{I_m(k_p R_{off}) I_1(k_p R_b)}{I_m(k_p a)} \Delta'_m(k_p a, k_p (R_{off} + R_b)) \Psi_{\perp}^{(p)}(\xi) + \right. \\ &\sum_{s=1} \frac{2v^2 D_2(\omega_s)}{a \omega_s^3 D'(\omega_s)} \frac{I_m(\kappa_{ps} R_{off}) I_1(\kappa_{ps} R_b)}{I_m^2(\kappa_{ps} a)} \times \\ &\left. I'_m(\kappa_{ps} (R_{off} + R_b)) \Psi_{\perp}^{(s)}(\xi) \right), \end{aligned} \quad (23)$$

$$\begin{aligned} \frac{F_z(r = R_{off} - R_b, \varphi, \xi)}{q} &= -\frac{4Q_b}{R_b L_b} \sum_{m=-\infty}^{+\infty} e^{im\varphi} \times \\ &\left( \frac{I_m(k_p (R_{off} - R_b)) I_1(k_p R_b)}{I_m(k_p a)} \Delta_m(k_p a, k_p R_{off}) \Psi_{\parallel}^{(p)}(\xi) + \right. \\ &\sum_{s=1} \frac{2v D_2(\omega_s)}{a \kappa_{ps} \omega_s^2 D'(\omega_s)} \frac{I_m(\kappa_{ps} R_{off}) I_1(\kappa_{ps} R_b)}{I_m^2(\kappa_{ps} a)} \times \\ &\left. I_m(\kappa_{ps} (R_{off} - R_b)) \Psi_{\parallel}^{(s)}(\xi) \right), \end{aligned} \quad (24)$$

$$\begin{aligned} \frac{F_r(r = R_{off} - R_b, \varphi, \xi)}{q} &= \frac{4Q_b}{R_b L_b} \sum_{m=-\infty}^{+\infty} e^{im\varphi} \times \\ &\left( \frac{I'_m(k_p (R_{off} - R_b)) I_1(k_p R_b)}{I_m(k_p a)} \Delta_m(k_p a, k_p R_{off}) \Psi_{\perp}^{(p)}(\xi) + \right. \\ &\sum_{s=1} \frac{2v^2 D_2(\omega_s)}{a \omega_s^3 D'(\omega_s)} \frac{I_m(\kappa_{ps} R_{off}) I_1(\kappa_{ps} R_b)}{I_m^2(\kappa_{ps} a)} \times \\ &\left. I'_m(\kappa_{ps} (R_{off} - R_b)) \Psi_{\perp}^{(s)}(\xi) \right), \end{aligned} \quad (25)$$

where  $Q_b$  is the bunch charge,  $L_b$  is the bunch length. It is important to note that for the last one integration a method of a waveguide structure excitation by an off-axis beam, well known in the theory of gyrotrons, was used. This method of integration consists in the transition from the laboratory frame of reference to the frame of reference with the origin located in the center of the beam. A detailed description of this method can be found, for example, in the paper [19]. The functions  $\Psi_{\parallel}^{p,s}(\xi)$  and  $\Psi_{\perp}^{p,s}(\xi)$  describe the axial structure of the wakefield:

$$\begin{aligned} \Psi_{\parallel}^{p,s}(\xi) &= \theta(\xi) \sin \omega_{p,s} \xi - \\ &\theta(\xi - L_b/v) \sin \omega_{p,s} (\xi - L_b/v), \\ \Psi_{\perp}^{p,s}(\xi) &= \theta(\xi) (1 - \cos \omega_{p,s} \xi) - \\ &\theta(\xi - L_b/v) (1 - \cos \omega_{p,s} (\xi - L_b/v)). \end{aligned} \quad (26)$$

The analytical expressions (22)–(25) allow to carry out a numerical analysis of the amplitudes distribution of the axial and radial forces acting on the particles that are on the envelope of the drive bunch, which is injected with the offset.

#### IV. NUMERICAL ANALYSIS RESULTS

Based on the derived wakefield excitation theory a numerical analysis was performed for the waveguide parameters in the terahertz frequency range, for the drive bunch we used parameters of electron bunches accessible at SLAC. These parameters are presented in Table I. First of all numerical methods were used to solve disper-

TABLE I. Parameters of the plasma–dielectric waveguide and the drive electron bunch

Parameter	Value
Inner dielectric radius	0.5 mm
Outer dielectric radius	0.6 mm
Permittivity of the dielectric	3.75 (quartz)
Plasma density	$4.41 \cdot 10^{14} \text{ cm}^{-3}$
Energy of bunch	5 GeV
Charge of bunch	3 nC
Length of bunch	5.0 mm
Radius of bunch	0.23 mm
Bunch offset	0.24 mm

sion equations for resonant  $TM$ -modes (which are chosen as the working modes for the accelerator structures) and hybrid electromagnetic  $HEM$ -modes (which are parasitic because of their excitation the BBU instability). For the parameters of the waveguide under present study and the electron 5 GeV drive bunch, the resonant frequencies of the first six eigen  $TM$ -modes are equal to 0.357 THz, 1.160 THz, 1.898 THz, 2.774 THz, 3.663 THz and 4.558 THz, respectively. The resonant frequencies of the first six eigen  $HEM$ -modes are 0.025 THz, 0.356 THz, 0.532 THz, 1.066 THz, 1.387 THz and 1.903 THz, respectively. In Fig.2 the longitudinal distributions of the axial and



radial forces behind the drive bunch acting on its particles are presented. The axial distributions in Fig.2 are shown along a line parallel to the structure axis and located at distances from it: (I) 0.47 mm, corresponding to the envelope of the drive bunch closer to the dielectric, and (II) 0.01 mm - the envelope of the drive bunch closer to the axis. As it can be seen from Fig.2 the radial force profile has an almost harmonic dependence on the longitudinal coordinate with a period approximately equal to the plasma wavelength. Thus the plasma wave makes a

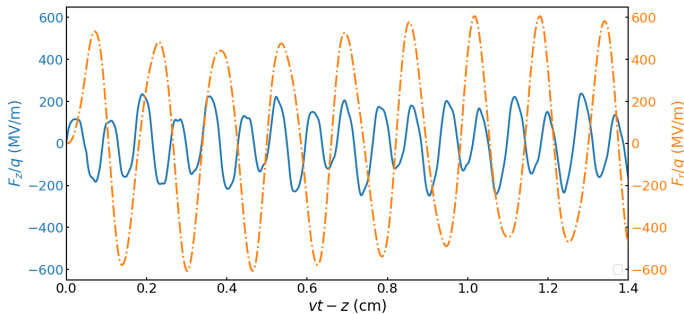


FIG. 2. The longitudinal profiles of the axial (solid line) and radial (dashed line) forces, excited by the off-axis drive electron bunch, at the distance 0.47 mm from the waveguide axis. Drive bunch of 0.5 mm length moves from right to left, a position of the bunch head corresponds to  $vt - z = 0$ .

predominant contribution to the radial force. The low-frequency modulation of the radial force amplitude is due to the excitation of the eigenwaves of the plasma-dielectric accelerating structure. At the same time, its contribution to the longitudinal force acting on the drive bunch particles located near the dielectric is insignificant. However it should be noted that by changing the plasma density it is possible to change the ratio between the amplitude of the plasma wave and the amplitudes of the eigenwaves of the excited structure. Fig.3 presents the distribution of radial forces behind the drive bunch acting on its peripheral particles. Fig.3 demonstrates the fact that the radial dynamics of the drive bunch par-

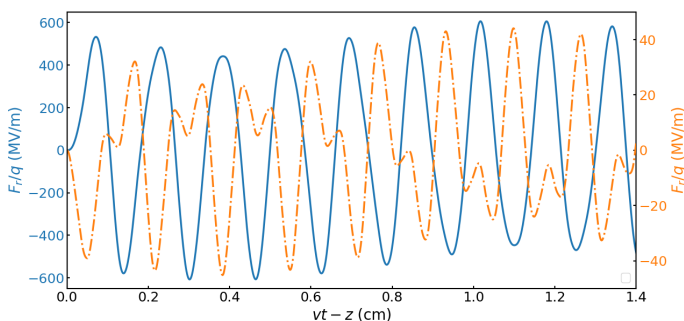


FIG. 3. The axial profiles of the radial force behind the off-axis drive bunch at the distances of 0.47 mm (solid line), and 0.01 mm (dashed line) from the axis of the waveguide. Drive bunch of 0.5 mm length moves from right to left, a position of the bunch head corresponds to  $vt - z = 0$ .

ticles located on its opposite transverse peripheries will differ as qualitatively as quantitatively. The bunch particles which are closer to the plasma-dielectric interface will focus in the axial direction during propagation along the accelerating structure. The focusing force increases along the bunch from its head to tail. The bunch particles which are closer to the waveguide axis, on the contrary, will defocus during propagation. The defocusing force also increases along the bunch from its head to tail. As a result, in the process of wakefield excitation the off-axis drive bunch will not deposit on the dielectric surface. And instead of a transverse displacement gradual increase there will be radial compression of the tail part of the bunch. The longitudinal profiles of the radial force was also compared for the case of a filling the channel for charged particles with plasma and the case of plasma absence in the channel. The results of this comparison are shown in Fig.4. In the absence of

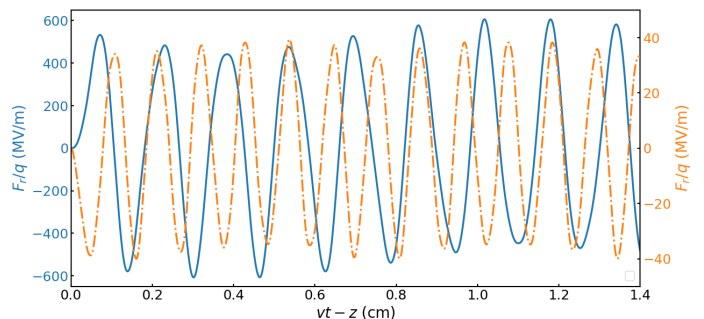


FIG. 4. The longitudinal profiles of the radial force behind the off-axis drive bunch at a distance of 0.47 mm from the axis of the waveguide in the case of filling the channel with plasma (solid line), and the absence of plasma in the channel (dashed line). Drive bunch of 0.5 mm length moves from right to left, a position of the bunch head corresponds to  $vt - z = 0$ .

plasma the off-axis drive bunch leads to significant excitation of *HEM*-modes with an azimuthal index  $m = 1$  (dipole modes). The analysis showed that these eigenmodes make a dominant contribution to the radial force, under the action of which the drive bunch particles will gradually move to the dielectric. The main reason of the difference between the amplitudes and the axial profiles of the radial forces for cases of presence and absence of the plasma is a plasma wave excitation by the drive bunch. The radial electric field of this wave acts on the bunch particles as a focusing system. Which, in turn, leads to a significant (qualitative and quantitative) change in the transverse dynamics of the drive bunch. Thus, it is possible to make a conclusion that the presence of the plasma in the channel for charged particles leads to the suppression of the transverse instability of the drive bunch. In turn, from a practical point of view, this will lead to: (I) prevent the charge losses of the drive bunch which excites the wakefield, (II) reduce the requirements for an injection accuracy, (III) increase the acceleration length of the witness bunch and, consequently, increase its output energy.

## V. CONCLUSIONS

An analytical theory of wakefield excitation by the off-axis particle bunch in the round plasma–dielectric waveguide has been formulated. A comparison of the longitudinal profiles of the axial and radial forces, excited by the off-axis drive electron bunch for the cases of the absence and presence of plasma in the channel for charged particles is carried out. It has been demonstrated that for the plasma–dielectric accelerating structure (unlike the

dielectric–loaded structure without plasma filling) the presence of the initial bunch offset does not lead to the beam breakup instability.

## ACKNOWLEDGMENTS

The study is supported by the National Research Foundation of Ukraine under the program “Leading and Young Scientists Research Support” (project # 2020.02/0299).

- 
- [1] M. C. Thompson, H. Badakov, A. M. Cook, J. B. Rosenzweig, R. Tikhoplav, G. Travish, I. Blumenfeld, M. J. Hogan, R. Ischebeck, N. Kirby, R. Siemann, D. Walz, P. Muggli, A. Scott, and R. B. Yoder, Breakdown limits on gigavolt-per-meter electron-beam-driven wakefields in dielectric structures, *Phys. Rev. Lett.* **100**, 214801 (2008).
- [2] B. D. O’Shea, G. Andonian, S. K. Barber, K. L. Fitzmorris, S. Hakimi, J. Harrison, P. D. Hoang, B. Naranjo, O. B. Williams, V. Yakimenko, and J. B. Rosenzweig, Observation of acceleration and deceleration in gigaelectron-volt-per-metre gradient dielectric wakefield accelerators, *Nature Communications* **7**, 1 (2016).
- [3] Q. Gao, G. Ha, C. Jing, S. P. Antipov, J. G. Power, M. Conde, W. Gai, H. Chen, J. Shi, E. E. Wisniewski, D. S. Doran, W. Liu, C. E. Whiteford, A. Zholents, P. Piot, and S. S. Baturin, Observation of high transformer ratio of shaped bunch generated by an emittance-exchange beam line, *Phys. Rev. Lett.* **120**, 114801 (2018).
- [4] K.-Y. Ng, Wake fields in a dielectric-lined waveguide, *Phys. Rev. D* **42**, 1819 (1990).
- [5] M. Rosing and W. Gai, Longitudinal and Transverse Wake Field Effects in Dielectric Structures, *Phys. Rev. D* **42**, 1829 (1990).
- [6] E. Garate, Transverse wake fields due to nonaxisymmetric drive beams in the dielectric wake-field accelerator, *Physics of Fluids B: Plasma Physics* **3**, 1104 (1991), <https://doi.org/10.1063/1.859838>.
- [7] W. Gai, A. D. Kanareykin, A. L. Kustov, and J. Simpson, Numerical simulations of intense charged-particle beam propagation in a dielectric wake-field accelerator, *Phys. Rev. E* **55**, 3481 (1997).
- [8] S. Y. Park and J. L. Hirshfield, Theory of wakefields in a dielectric-lined waveguide, *Phys. Rev. E* **62**, 1266 (2000).
- [9] S. Y. Park and J. L. Hirshfield, Bunch stability during high-gradient wakefield generation in a dielectric-lined waveguide, *Physics of Plasmas* **8**, 2461 (2001), <https://doi.org/10.1063/1.1343886>.
- [10] C. Li, W. Gai, C. Jing, J. G. Power, C. X. Tang, and A. Zholents, High gradient limits due to single bunch beam breakup in a collinear dielectric wakefield accelerator, *Phys. Rev. ST Accel. Beams* **17**, 091302 (2014).
- [11] V. Lebedev, A. Burov, and S. Nagaitsev, Efficiency versus instability in plasma accelerators, *Phys. Rev. Accel. Beams* **20**, 121301 (2017).
- [12] V. E. Balakin, A. V. Novokhatsky, and V. Smirnov, VLEPP: Transverse beam dynamics, in *12th International Conference on High Energy Accelerators*, Vol. 830811, edited by F. T. Cole and R. Donaldson (Fermilab, Batavia, IL, 1983) pp. 119–120.
- [13] D. Y. Shchegolkov, E. I. Simakov, and A. A. Zholents, Towards a practical multi-meter long dielectric wakefield accelerator: Problems and solutions, *IEEE Transactions on Nuclear Science* **63**, 804 (2016).
- [14] S. S. Baturin and A. Zholents, Stability condition for the drive bunch in a collinear wakefield accelerator, *Phys. Rev. Accel. Beams* **21**, 031301 (2018).
- [15] G. Sotnikov, K. Galaydych, R. Kniaziev, and I. Onishchenko, BBU instability in rectangular dielectric resonator, *Journal of Instrumentation* **15** (05), C05034.
- [16] R. D. Ruth, A. W. Chao, P. L. Morton, and P. B. Wilson, A PLASMA WAKE FIELD ACCELERATOR, Part. Accel. **17**, 171 (1985).
- [17] J. B. Rosenzweig, B. Breizman, T. Katsouleas, and J. J. Su, Acceleration and focusing of electrons in two-dimensional nonlinear plasma wake fields, *Phys. Rev. A* **44**, R6189 (1991).
- [18] G. V. Sotnikov, R. R. Kniaziev, O. V. Manuilenko, P. I. Markov, T. C. Marshall, and I. N. Onishchenko, Analytical and numerical studies of underdense and overdense regimes in plasma-dielectric wakefield accelerators, *Nucl. Instrum. Meth. A* **740**, 124 (2014).
- [19] K. Chu and A. Lin, Gain and bandwidth of the gyro-twt and carm amplifiers, *IEEE Transactions on Plasma Science* **16**, 90 (1988).